Constraining the Dielectric Permittivities of the Moon's Subsurface Using Physics Informed Deep Learning

Zi Xian Leong (zxleong@psu.edu) and Tieyuan Zhu,
The Pennsylvania State University, Department of Geosciences, University Park, PA, United States

Summary

The deeper subsurface layers beyond the lunar regolith are not well-constrained. Using in-situ lunar penetrating radar data (*d*) from Change'E-3 Yutu rover, we invert for its subsurface relative dielectric permittivity (ε_r) model.

We use a physics informed convolutional neural network (CNN) based deep learning architecture to regress the relationship between ε_r – *d*. We incorporate a priori physics knowledge such as known lunar ε_r estimates [1-9] and attenuation during the generation of synthetic training dataset.

In total, we trained 20 (iterations) neural network models and averaged the predictions to make a final predicted ε_r model as well as calculating the model's uncertainties.

We validate our physics informed deep learning approach by comparing the predicted forward data from ε_r estimates to the field data.

Our interpretation suggests multiple layers in the upper 200 meters in the order of regolith, ejectas, Eratosthenian basaltic lava flows, paleoregolith, and lava flows from Imbrium period.

Workflow

Our workflow is organized as follows:

1. We simulate 15,000 random synthetic ε_r and its corresponding radargram using reflectivity method by Kennett (1983) (Fig 1). The synthetic ε_r are generated based on ranges of 1 – 9 (Zhu et al., 2021)
2. We incorporate radar attenuation (Lai et al., 2020) as means to augment our dataset (Fig 2). The attenuation (α) equation is $\alpha = \frac{2\pi}{\lambda}\sqrt{\varepsilon_r}\left[\frac{1}{2}\left(\sqrt{1+\tan^2\delta}-1\right)\right]^{1/2}$; where λ is the wavelength in the medium, $tan\,\delta$ is the loss tangent (0.006). We apply attenuation to the radargram by $De^{k*\alpha*t}$; where D_{attn} is the augmented radargram with attenuation, D is original radargram, k is a scaling coefficient which is randomized during augmentation, t is the time steps. In total, we generated 75,000 datasets.
3. Our CNN is based on Leong and Zhu (2021), in which input is radargram and output is corresponding ε_r. Here, we add two more layers at the Atrous Spatial Pyramid Pooling (ASPP) module to encourage more contextual feature learning (Fig 3).
4. We train the neural network 20 times, each time yielding different results due to the stochastic randomness from the convolutional layers within the neural network. From the 20 models, the averaged predictions is taken as the final ε_r prediction along with its uncertainties. (Figs 4 – 10).

Workflow Figures

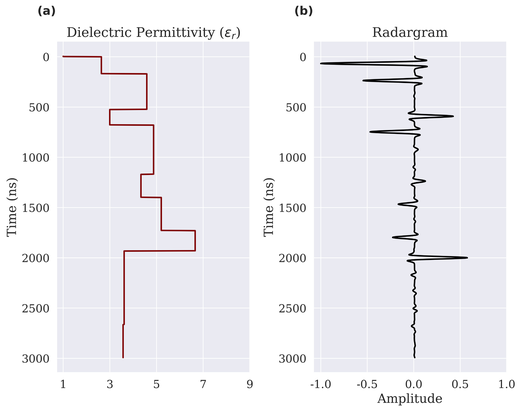

Fig. 1: (a) example of relative dielectric permittivity, ε_r, while (b) is its corresponding radargram.

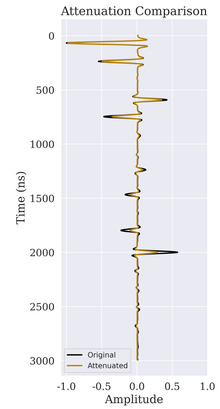

Fig. 2: Example of radargram with attenuation.

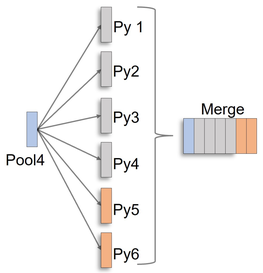

Fig. 3: We added two more layers at the ASPP module, as depicted in the orange modules (grey modules are originally from Leong and Zhu, 2021). The ASPP uses Atrous convolution instead of a vanilla convolution, which allows for an enlarged field of view during convolution. This is especially useful in the encoding of the input data (LPR data) because a wider convolution window enables more neighboring information to be encoded. For example, the reflection energy recorded at an interface often contains leftover energy around the reflection time depth due to nature of the source wavelet and/or energy from multiples.

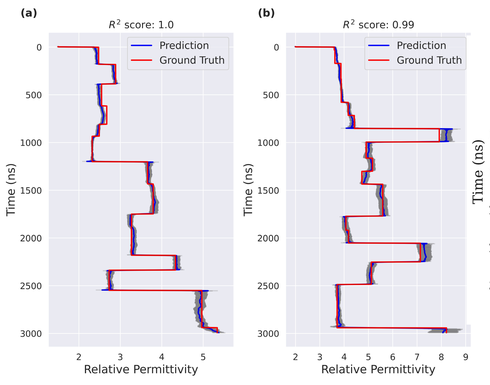

Fig. 4: Examples of synthetic ε_r predictions compared with ground truth. The dark shaded area are the uncertainties (standard deviation) calculated from the 20 trained models. The blue lines represent the ε_r predictions, while red lines are the corresponding ground truths.

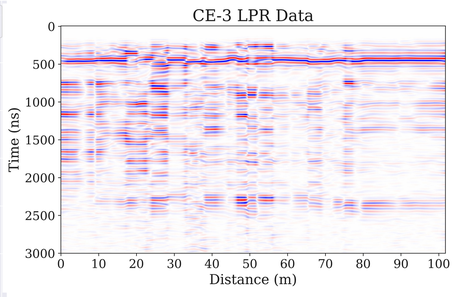

Fig. 5: Preprocessed Chang'E-3 (CE-3) lunar penetrating radar (LPR) data from Yutu rover. Preprocessing is done by closely following the steps taken in Zhu et al., 2021.

Dielectric Permittivity Predictions & Evaluation

Fig. 6: Two examples of ε_r predictions on CE-3 LPR Data.

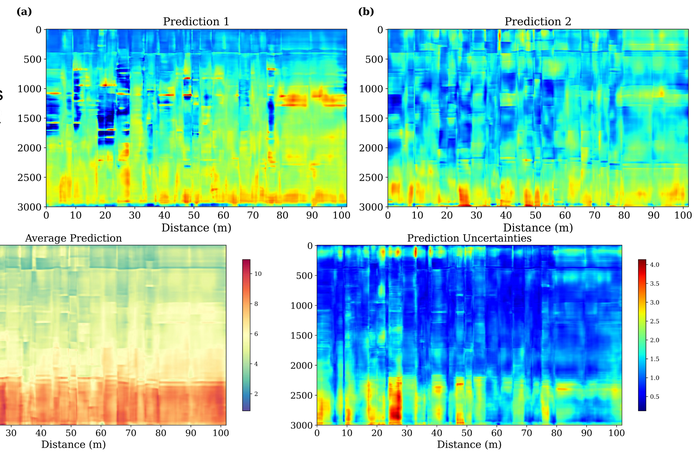

Fig. 7: Average ε_r from the 20 predictions.

Fig. 8: Uncertainties (standard deviation) from the 20 predictions.

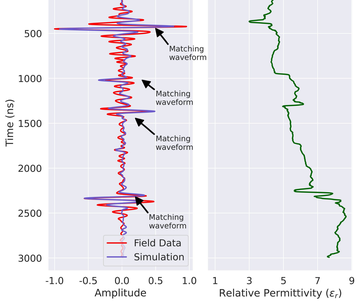

Fig. 9: Comparison of predicted forward data and original CE-3 LPR data.

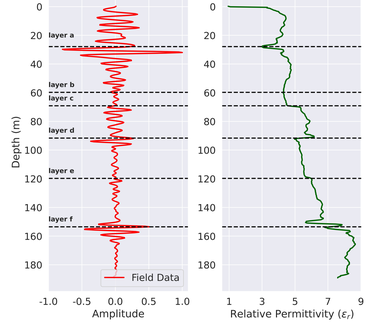

Fig. 10: *Layer a* is regolith, *b* is ejectas with Eratosthenian basalt, *c* is paleoregolith, *d* is ejectas and paleoregolith mix, and *layers e and f* are lava flows from Imbrium period.

Discussion & Future Work

- Our results seem reasonable considering the fitting match between predicted forward data and field data.
- We are currently working on LPR data from Yutu-2 rover from Chang'E-4 spacecraft.

Acknowledgement

We thank PSU's Environment Geophysics Group (https://sites.psu.edu/tzhu/) and Shell US (Geosciences Energy Research Facilitation Award) for funding this research. We also thank the Chinese National Space Agency (CNSA) for providing the CE-3 LPR data.